High-Resolution Structure of the Photosynthetic Mn_4Ca Catalyst from X-ray Spectroscopy

Junko Yano[1,2], Jan Kern[3], Yulia Pushkar[1,2], Kenneth Sauer[1,2], Pieter Glatzel[4], Uwe Bergmann[5], Johannes Messinger[6], Athina Zouni[3], Vittal K. Yachandra[1]

[1]*Melvin Calvin Laboratory, Physical Biosciences Division, Lawrence Berkeley National Laboratory, Berkeley, CA 94720, USA*

[2]*Department of Chemistry, University of California, Berkeley, CA 94720, USA*

[3]*Max-Volmer-Laboratorium für Biophysikalische Chemie, Technische Universität, D-10623 Berlin, Germany*

[4]*European Synchrotron Radiation Facility, F-38043 Grenoble Cedex, France*

[5]*Stanford Synchrotron Radiation Laboratory, Menlo Park, CA 94305, USA*

[6]*Max-Planck-Institut für Bioanorganische Chemie, D-45470 Mülheim an der Ruhr, Germany*

To whom correspondence should be addressed: vkyachandra@lbl.gov

Keywords: EXAFS, manganese, oxygen-evolving complex, polarized EXAFS, photosystem II, PS II single crystals, RIXS, XANES, XAS, X-ray absorption spectroscopy

Abstract

The application of high-resolution X-ray spectroscopy methods to study the photosynthetic water oxidizing complex, which contains a unique hetero-nuclear catalytic Mn_4Ca cluster, are described. Issues of X-ray damage especially at the metal sites in the Mn_4Ca cluster are discussed. The structure of the Mn_4Ca catalyst at high-resolution which has so far eluded attempts of determination by X-ray diffraction, EXAFS and other spectroscopic techniques has been addressed using polarized EXAFS techniques applied to oriented PS II membrane preparations and PS II single crystals. A review of how the resolution of traditional EXAFS techniques can be improved, using methods such as range-extended EXAFS is presented, and the changes that occur in the structure of the cluster as it advances through the catalytic cycle are described. X-ray absorption and emission techniques (XANES and Kβ emission) have been used earlier to determine the oxidation states of the Mn_4Ca cluster, and in this report we review the use of X-ray resonant Raman spectroscopy to understand the electronic structure of the Mn_4Ca cluster as it cycles through the intermediate S-states.

1. Introduction

Life on Earth relies on oxygen, and only because of the constant regeneration of oxygen through photosynthetic water oxidation by green plants, cyanobacteria and algae is it abundant in the atmosphere. The structure of the catalytic Mn_4Ca complex, that oxidizes H_2O to O_2 and is part of a multi-protein membrane system known as photosystem II (PS II), has been the subject of intense study ever since Mn was identified as an essential element for oxygenic photosynthesis (Wydrzynski & Satoh 2005). Water oxidation in PS II is a stepwise process wherein each of 4 sequential photons absorbed by the reaction center powers the advance of the oxygen-evolving complex (OEC) through the S-state intermediates, S_0 through S_4 (Kok et al. 1970). Upon reaching the S_4 state, the complex releases O_2 and returns to S_0. The critical questions related to this process are the structural and electronic state changes in the Mn_4Ca complex as the OEC proceeds through the S-state cycle. The recent results from our laboratory that address these questions, using polarized EXAFS of single crystals of PS II (Yano et al. 2005a; Yano et al. 2006), range-extended EXAFS (Pushkar et al. 2006; Yano et al. 2005b), and X-ray Raman spectroscopy or resonant inelastic X-ray spectroscopy (RIXS) (Glatzel et al. 2004; Glatzel et al. 2005), were presented at the Royal Society Discussion meeting on 'Revealing how nature uses sunlight to split water' and are reviewed here.

2. Structure of the Mn_4Ca Cluster in Photosynthesis

a) Single Crystal X-ray Spectroscopy

A key to understanding the mechanism of water oxidation by the OEC in PS II is the determination of the structure of the Mn_4Ca cluster, which has eluded both Mn X-ray absorption fine structure (EXAFS) (Dau et al. 2001; Penner-Hahn 1998; Sauer et al. 2007; Yachandra 2005)

and X-ray diffraction (XRD) studies (Ferreira et al. 2004; Kamiya & Shen 2003; Loll et al. 2005; Zouni et al. 2001) until now. Availability of PS II single-crystals and the X-ray crystallography studies of PS II have opened up the possibility of using spectroscopic studies of single crystals to obtain a detailed high-resolution structure of the catalytic site of water oxidation in PS II.

Damage by X-rays: A Case Study for Metallo-Protein Crystallography. In order to determine a safe level of X-ray dose for our single-crystal X-ray spectroscopy studies, we conducted a comprehensive survey of the effects of radiation dose, energy of the X-rays, and temperature on the structure of the Mn_4Ca cluster in single-crystals and solutions of PS II. These studies (Yano et al. 2005a) have revealed that the conditions used for structure determination by X-ray diffraction methods are damaging to the metal-site structure as monitored by XANES and EXAFS spectroscopy, for both cyanobacteria and spinach at room and lower temperatures (Grabolle et al. 2006; Yano et al. 2005a). With the advent of third-generation synchrotron sources, the intensity of X-rays available for crystallography has increased considerably, and X-ray damage to biomolecules has been a continuing concern. This is a well recognized problem, and various steps have been taken to minimize such damage (Garman 2003). In most crystallography studies it is the loss of diffractivity as evidenced by loss of resolution that is used as a measure of X-ray damage (Henderson 1990). However, as shown in our study (Yano et al. 2005a), this method is not sensitive to localized damage as is prevalent in redox-active metal containing proteins. We used *in situ* XANES and EXAFS to show that for the Mn_4Ca cluster in PS II the damage to the metal site precedes the loss of diffractivity by more than an order of magnitude of X-ray dose. This case study demonstrates that such *in situ* evaluation of the structural intactness of the active site(s) by spectroscopic techniques can be critical to validate structures derived from crystallography. Since structure-function correlations are routinely made

using the structures determined by X-ray crystallography, it is important to know that the metal-site structures are indeed intact. This is particularly important for radiation-sensitive metallo-proteins.

Although X-ray crystallography studies of PS II have added valuable information to our knowledge about the location of the Mn_4Ca cluster, at present there are serious discrepancies among the structural models for the Mn_4Ca complex derived from these studies, and inconsistencies with spectroscopic data. This disagreement is probably a consequence of both X-ray-induced damage to the catalytic metal site and differences in the interpretation of the electron density at the presently available resolution (3.0 to 3.8 Å) (Ferreira et al. 2004; Kamiya & Shen 2003; Loll et al. 2005; Zouni et al. 2001).

The Mn XANES data from PS II single crystals show that following X-ray doses characteristic of the XRD measurements, Mn is reduced to Mn(II) from $Mn_4(III_2,IV_2)$ present in the S_1-state (Fig. 1 left). Moreover, the EXAFS spectrum changes significantly, from one that is characteristic of a multinuclear oxo-bridged Mn_4Ca complex to one that is typical of mononuclear hexa-coordinated Mn(II) in solution (Fig. 1 right) (Yano et al. 2005a). These X-ray spectroscopy results present clear evidence that there are no specific metal-bridging or metal-metal interactions, as shown by the disappearance of the Fourier peaks that are characteristic of Mn-bridging oxo, and Mn-Mn/Mn-Ca interactions with di-μ-oxo or mono μ-oxo bridges, and by the appearance of Mn-O distances characteristic of Mn(II)-O ligand bond lengths. The density seen in the X-ray diffraction results is in all probability from the Mn(II)-hexa coordinated ions that are distributed in the binding pocket, presumably bound to carboxylate ligands and free water, leading to a distribution of metal binding sites and the resultant unresolved electron density. It is not necessary for the metal ions to move away from the site, just that they are all

bound in a distribution of sites, without the presence of di- or mono μ-oxo bridged Mn-Mn or Mn-Ca units.

These studies reveal that the conditions used for structure determination by X-ray crystallography cause serious damage specifically to the metal-site structure, and they provide quantitative details. The results show furthermore that the damage to the active metal site occurs at a much lower X-ray dose than that causing the loss of diffractive power of the crystals as established by X-ray crystallography. The damage is significantly higher at wavelengths used for anomalous diffraction measurements and is much lower at liquid He temperatures (10 K) compared to 100 K, where the crystallography experiments were conducted. For future X-ray crystallography work on the Mn_4Ca complex it will therefore be imperative to develop protocols that mitigate the X-ray induced damage. More generally, these data show that in redox-active metalloproteins careful evaluations of the structural intactness of the active site(s) is required before structure-function correlations can be made on the basis of high resolution X-ray crystal structures.

Structure of the Mn_4Ca Complex from Polarized EXAFS of PS II Crystals PS II membranes can be oriented on a substrate such that the membrane planes are roughly parallel to the substrate surface. This imparts a one-dimensional order to these samples; while the *z* axis for each membrane (collinear with the membrane normal) is roughly parallel to the substrate normal, the *x* and *y* axes remain disordered (Rutherford 1985). Exploiting the plane-polarized nature of synchrotron radiation, spectra can be collected at different angles between the substrate normal and the X-ray **e**-vector. The dichroism of the absorber-backscatterer pair present in the oriented samples is reflected in, and can be extracted from, the resulting X-ray absorption spectra (Cinco et al. 2004; Dau et al. 1995; Dau et al. 2001; George et al. 1989; Mukerji et al. 1994). The

EXAFS of the oriented PS II samples exhibits distinct dichroism, from which we have deduced the relative orientations of several interatomic vector directions relative to the membrane normal and derived a topological representation of the metal sites in the OEC. However, because the samples are ordered in only one dimension, the dichroism information is available only in the form of an angle with respect to the membrane normal. For EXAFS measurements, this means that the absorber-backscatterer vectors can lie anywhere on a cone defined by the angle the vector forms with the membrane normal.

Further refinement can be performed if samples with three-dimensional order, *i.e.* single crystals, are examined instead of oriented membranes (Flank et al. 1986; Scott et al. 1982). This is possible because the EXAFS amplitude is proportional to $\sim\cos^2\theta$, where θ is the angle between the X-ray *E* vector and the absorber-backscatterer vector. These studies have been able to significantly expand the X-ray absorption spectroscopic information available for these systems over what is gleaned from studies of isotropic samples. We have developed the methodology for collecting single-crystal XAS data from PS II. XAS spectra were measured at 10 K using a liquid He cryostat or cryostream, and an imaging plate detector placed behind the sample was used for *in situ* collection of diffraction data and determination of the crystal orientation.

We have reported the polarized EXAFS spectra of oriented PS II single crystals, which result in a set of four similar high-resolution structures for the Mn_4Ca cluster (Fig. 2A) (Yano et al. 2006), which were derived from simulations of single-crystal polarized spectra based on the experimentally observed dichroism. These structural models are dependent only on the spectroscopic data, and are independent of the electron density from X-ray diffraction studies. The structure of the Mn_4Ca cluster from the polarized EXAFS study of PS II single crystals is unlike either the 3.0 (Loll et al. 2005) or 3.5 Å (Ferreira et al. 2004) resolution X-ray structures,

and other previously proposed models. The structure of the Mn_4Ca cluster favoured in our study contains structural features that are unique and are likely to be important in facilitating water-oxidation chemistry.

In order to discriminate between symmetry-related structural models that are possible because of the presence of a non-crystallographic C_2 axis, the cluster was placed within PS II taking into account the overall shape of the electron density of the metal site and the putative ligand information from X-ray crystallography, including IR and EPR studies. The center of mass of the structural models was translated to the center of electron density attributed to the Mn_4Ca cluster in the 3.0 Å XRD structure (Loll et al. 2005) and the models were not optimized with respect to the electron density, or rotated with respect to the crystal axes, as that would change the dichroic characteristics. Of the four options shown in Fig. 2A, it is possible to rule out Model I on the basis of oriented membrane EXAFS data (Cinco et al. 2004; Pushkar et al. 2007). Model II, IIa and III in the putative ligand environment are shown in Fig. 2B. However, we caution that the ligand positions are tentative because they are likely to be affected by radiation damage, as are the positions of the metals atoms from XRD (Grabolle et al. 2006; Yano et al. 2005a).

The polarized EXAFS study of PS II single crystals demonstrates that the combination of XRD and polarized EXAFS has several advantages for unraveling structures of X-ray damage-prone, redox-active metal sites in proteins. XRD structures at medium resolution are sufficient to determine the overall shape and placement of the metal site within the ligand sphere, and refinement using polarized EXAFS can provide accurate metal-metal/ligand vectors. In addition, we are extending the study to determine the structure of the Mn_4Ca cluster in the intermediate S-states of the OEC, which are difficult to study with XRD at high resolution.

b) <u>Range-extended X-ray absorption Spectroscopy</u>

EXAFS spectra of metallo-protein samples are normally collected as an excitation spectrum by electronically windowing the Kα emission (2p to 1s) from the metal atom (Cramer 1988; Scott 1984; Yachandra 1995). The solid-state detectors used over the past decade have a resolution of 150-200 eV, making it impossible to discriminate the fluorescence of the absorbing atom (Mn in our case for PS II) from that of the following element (Fe in PS II) in the periodic table. The distances from Mn that can be resolved in a typical EXAFS experiment are given by $\Delta R=\pi/2\Delta k$, where k is the energy of the Mn photoelectron. Unfortunately, because of the presence of Fe in the PS II samples we have been limited to a Δk of about 12 $Å^{-1}$, that places an inherent limit on the resolution of Mn distances to about 0.14 Å. We have overcome this limitation by using a high resolution crystal monochromator (Bergmann & Cramer 1998), that has a resolution of 1 eV to collect EXAFS spectra well beyond the Fe K-edge to k=15 $Å^{-1}$, thus improving the distance resolution to 0.09 Å (Fig. 3A). We have recently shown the feasibility of the range-extended EXAFS method and collected data without interference from Fe in the sample (Yano et al. 2005b).

We can now resolve two short Mn-Mn distances in the S_1 and S_2 states; while earlier we could discern only one distance of ~2.7 Å. We have also collected range-extended polarized EXAFS data using oriented PS II membranes, and it is quite clear that the heterogeneity is more obvious; the Mn-Mn distance is ~2.7 Å or 2.8 Å depending on the angle the X-ray **e**-vector makes with the membrane normal. Interestingly, for the first time we were able to resolve the FT peak at ~3.3 Å into one Mn-Mn vector at 3.3 Å and two Mn-Ca vectors at 3.4 Å, that are aligned at different angles to the membrane normal (Pushkar et al. 2006).

In Fig. 3B Fourier transforms (FTs) of the range-extended EXAFS for PS II in isotropic solution and in oriented membranes in S_1 state are compared. Peaks, labeled I, II, III corresponding to the shells of backscatterers from the Mn absorber. Peak I contains Mn-O bridging and terminal interactions, peak II corresponds to di-μ-oxo-bridged Mn-Mn moieties, peak III has information about mono-μ-oxo-bridged Mn-Mn and Mn-Ca interactions. Increased spectral resolution results in the detection of the orientation dependence of peaks II and III.

Figure 3C shows polar plots of the N_{app} plotted (solid circles) with respect to detection angle (θ). By fitting the angle dependence of the amplitude (N_{app}) to equation (1),

$$N_{app}(\theta) = N_{iso} + \frac{1}{2} N_{iso}(3\cos^2\theta - 1)(3\cos^2\phi - 1) I_{ord} \qquad (1)$$

the approximate number of backscatterers (N_{iso}) and the average orientation $<\phi>$ for that shell of scatterers can be determined. Analysis of the orientation dependence of the ~2.7 Å Mn-Mn vector results in two Mn-Mn interactions at an average angle of $<\phi> = 61\pm5°$, with respect to the membrane normal. The ~2.8 Å Mn-Mn vector has one Mn-Mn interaction at an angle of $<\phi> = 64\pm10°$ with respect to the membrane normal. In this way we independently derived that the three Mn-Mn distances of ~ 2.7 Å and ~ 2.8 Å are present in a 2:1 ratio in PS II samples in the S_1 state.

The range-extended EXAFS method allowed us to resolve the complex nature of the Peak III containing at least two peaks, IIIA and IIIB, having different distances of 3.2 Å and 3.4 Å. Previous Ca EXAFS studies of native PS II (Cinco et al. 2002), Sr EXAFS of Sr-substituted PS II (Cinco et al. 1998), and Mn EXAFS (Latimer et al. 1995) of Ca-depleted PS II (Latimer et al. 1998) have shown the contribution of both Mn-Mn (~3.2 Å) and Mn-Ca (~3.4 Å) vectors to FT peak III. Peak IIIB can be assigned to the Mn-Ca vector and peak IIIA to the Mn-Mn vector,

and moreover, the dichroic behavior of the peak IIIB, is strikingly similar to that reported previously for the Mn-Sr vector (Cinco et al. 2004).

We have extended these studies to the S_0 and S_3 intermediate states of the enzymatic cycle, and the preliminary results show that there is a significant change in the structure of the Mn complex in the S_3 state. This result has important implications for choosing between the many mechanisms that have been proposed for the water oxidation reaction. In conjunction with the data from single-crystal XAS studies, these studies promise to reveal the changes that occur in the structure of Mn_4Ca catalyst as it cycles through the S-states and the mechanism of water oxidation.

3. Electronic Structure of the Mn_4Ca Cluster

X-ray Resonant Raman or Resonant Inelastic X-ray Scattering (RIXS). A key question for the understanding of photosynthetic water oxidation is whether the four oxidizing equivalents generated by the reaction center are accumulated on the four Mn ions of the OEC during S-state turnover, or whether a ligand-centered oxidation takes place, especially, before the formation and release of molecular oxygen during the S_3 to (S_4) to S_0 transition (Yano & Yachandra 2007). It is crucial to solve this problem, because the Mn redox states form the basis for any mechanistic proposal. The description of the Mn_4Ca cluster in the various S-states in terms of the formal oxidation states is very useful, and Mn K-edge XANES has been the conventional X-ray spectroscopic method for determining the oxidation states. However, it is also important to understand the electronic structure of the Mn cluster in more detail, and we are using the technique of X-ray resonant Raman or X-ray inelastic scattering spectroscopy (RIXS) that has potential for addressing this issue. The RIXS data are collected by scanning the incident energy (1s to 3d/4p absorption followed by 2p-1s emission) to yield two-dimensional plots that can be

interpreted along the incident energy axis or the energy transfer axis, which is the difference between the incident and emission energies (Fig. 4A) (Glatzel & Bergmann 2005). This method provides a description of the degree of covalency and d-orbital occupancy of the Mn complex, both parameters that are critical for understanding what makes this cluster function as it advances through the enzymatic cycle.

We have compared the spectral changes in the RIXS spectra between the Mn_4Ca cluster in the S-states (Glatzel et al. 2004), Mn oxides (Glatzel et al. 2005), and Mn coordination complexes, and the results indicate clear differences in how the protein environment modulates the Mn atoms, leading to stronger covalency for the electronic configuration in the Mn_4Ca cluster compared to that in the oxides or coordination complexes.

The RIXS two-dimensional data are best shown as contour plots (Fig. 4B). The comparison of Mn(II), Mn(III), Mn(IV) and PS II in the S_1 and S_2 states shows that both states states contain a mixture of oxidation states Mn(III) and Mn(IV). The integrated cross sections along the Raman or energy transfer axis are the L_3-like edge (2p to 3d) (Fig. 4C, left). The integrated cross sections along the incident energy are the K-edge (1s to 3d) transition (Fig. 4C, right). It is clear from Fig. 4 that Mn in the S_1 state contains oxidation states III and IV; thus providing confirmation for the (III_2,IV_2) assignment for the S_1 state.

The 1st moment of the spectrum integrated along the incident energy axis (see Fig. 4B) was calculated for all the S-states and compared with the 1^{st} moments obtained from Mn oxides and Mn coordination compounds in formal oxidation states of (II), (III) and (IV).

The changes per oxidation state in the first moment positions are more pronounced between the Mn oxides than between the Mn coordination complexes. This observation is consistent with a stronger covalency in the coordination complexes. We furthermore observe a

Mn oxidation between the S_1 and S_2 states of PS II even though the change in the Mn electronic structure is less pronounced than in the oxides. The spectral change per Mn ion between $Mn^{III}(acac)_3$ and Mn^{IV}(salicylate) (bipy) is by a factor of 2 more pronounced than between S_1 and S_2. In other words, the orbital population change Δn_{3d}^{eff} per change in oxidation state is largest between the Mn oxides and smallest between S_1 and S_2. The reason is an increased covalency or delocalization of the Mn valence orbitals in the Mn_4Ca cluster in PS II. We thus find that the electron that is transferred from the OEC in PS II between S_1 and S_2 is strongly delocalized.

Although there has been general agreement with respect to the increasing oxidation of Mn in the cluster during S_0 to S_1 and S_1 to S_2, there is a lack of consensus concerning Mn oxidation during S_2 to S_3. It is also not clear whether the S_0 state contains any Mn(II). Recent preliminary results from the S_0 and S_3 states show that the orbital population change Δn_{3d}^{eff} per change in oxidation state between the S_2 and S_3 states is half as much as that between S_0 and S_1, or S_1 and S_2. These results indicate that the electron is removed from a more covalent form or a more delocalized orbital during the S_2 to S_3 transition compared to the S_0 to S_1 and S_1 to S_2 transitions.

These results are in agreement with the earlier qualitative conclusions derived from the shifts in the XANES inflection point energies and the Kβ emission peaks from the S-states and support considering a predominantly ligand-based oxidation during the S_2 to S_3 transition (Messinger et al. 2001; Yano & Yachandra 2007).

Acknowledgements

The research presented here was supported by the NIH Grant GM 55302 (VKY), and by the Director, Office of Science, Office of Basic Energy Sciences (OBES), Division of Chemical Sciences, Geosciences, and Biosciences of the Department of Energy (DOE) under Contract DE-AC02-05CH11231. Grant support from the Deutsche Forschungsgemeinschaft SFB 498, TP C7 to AZ, and Me 1629/2-4 and from the Max-Planck-Gesellschaft to JM are gratefully acknowledged. Synchrotron facilities were provided by the Stanford Synchrotron Radiation Laboratory (SSRL), the Advanced Light Source (ALS), and the Advanced Photon Source (APS) operated by DOE OBES. The SSRL Biomedical Technology program is supported by NIH, the National Center for Research Resources (NCRR), and the DOE Office of Biological and Environmental Research, and the BioCAT at APS is supported by NCRR.

References

Bergmann, U. & Cramer, S. P. 1998 A high-resolution large-acceptance analyzer for x-ray fluorescence and raman spectroscopy. In *Spie conference on crystal and multilayer optics*, vol. 3448, pp. 198-209. San Diego, CA: SPIE.

Cinco, R. M., Holman, K. L. M., Robblee, J. H., Yano, J., Pizarro, S. A., Bellacchio, E., Sauer, K. & Yachandra, V. K. 2002 Calcium exafs establishes the mn-ca cluster in the oxygen-evolving complex of photosystem ii. *Biochemistry* **41**, 12928-12933.

Cinco, R. M., Robblee, J. H., Messinger, J., Fernandez, C., Holman, K. L. M., Sauer, K. & Yachandra, V. K. 2004 Orientation of calcium in the mn4ca cluster of the oxygen-evolving complex determined using polarized strontium exafs of photosystem ii membranes. *Biochemistry* **43**, 13271-13282.

Cinco, R. M., Robblee, J. H., Rompel, A., Fernandez, C., Yachandra, V. K., Sauer, K. & Klein, M. P. 1998 Strontium exafs reveals the proximity of calcium to the manganese cluster of oxygen-evolving photosystem ii. *J. Phys. Chem. B* **102**, 8248-8256.

Cramer, S. P. 1988 Biochemical applications of x-ray absorption spectroscopy. In *X-ray absorption: Principles, applications and techniques of exafs, sexafs, and xanes* (ed. D. C. Koningsberger & R. Prins), pp. 257-326. New York: Wiley-Interscience.

Dau, H., Andrews, J. C., Roelofs, T. A., Latimer, M. J., Liang, W., Yachandra, V. K., Sauer, K. & Klein, M. P. 1995 Structural consequences of ammonia binding to the manganese cluster of the photosynthetic oxygen-evolving complex: An x-ray absorption study of isotropic and oriented photosystem ii particles. *Biochemistry* **34**, 5274-5287.

Dau, H., Iuzzolino, L. & Dittmer, J. 2001 The tetra-manganese complex of photosystem ii during its redox cycle - x-ray absorption results and mechanistic implications. *Biochim. Biophys. Acta* **1503**, 24-39.

Ferreira, K. N., Iverson, T. M., Maghlaoui, K., Barber, J. & Iwata, S. 2004 Architecture of the photosynthetic oxygen-evolving center. *Science* **303**, 1831-1838.

Flank, A. M., Weininger, M., Mortenson, L. E. & Cramer, S. P. 1986 Single-crystal exafs of nitrogenase. *J. Am. Chem. Soc.* **108**, 1049.

Garman, E. 2003 Cool crystals: Macromolecular cryocrystallography and radiation damage. *Curr. Opin. Struct. Biol.* **13**, 545-551.

George, G. N., Prince, R. C. & Cramer, S. P. 1989 The manganese site of the photosynthetic water-splitting enzyme. *Science* **243**, 789-791.

Glatzel, P. & Bergmann, U. 2005 High resolution 1s core hole x-ray spectroscopy in 3d transition metal complexes - electronic and structural information. *Coord. Chem. Rev.* **249**, 65-95.

Glatzel, P., Bergmann, U., Yano, J., Visser, H., Robblee, J. H., Gu, W. W., de Groot, F. M. F., Christou, G., Pecoraro, V. L., Cramer, S. P. & Yachandra, V. K. 2004 The electronic structure of mn in oxides, coordination complexes, and the oxygen-evolving complex of photosystem ii studied by resonant inelastic x-ray scattering. *J. Am. Chem. Soc.* **126**, 9946-9959.

Glatzel, P., Yano, J., Bergmann, U., Visser, H., Robblee, J. H., Gu, W., de Groot, F. M. F., Cramer, S. P. & Yachandra, V. K. 2005 Resonant inelastic x-ray scattering (rixs) spectroscopy at the mn k absorption pre-edge - a direct probe of the 3d orbitals. *J. Phys. Chem. Solid.* **66**, 2163-2167.

Grabolle, M., Haumann, M., Muller, C., Liebisch, P. & Dau, H. 2006 Rapid loss of structural motifs in the manganese complex of oxygenic photosynthesis by x-ray irradiation at 10-300 k. *J. Biol. Chem.* **281**, 4580-4588.

Henderson, R. 1990 Cryoprotection of protein crystals against radiation damage in electron and x-ray diffraction. *Philos. Trans. R. Soc. Lond. Ser. B-Biol. Sci.* **241**, 6-8.

Kamiya, N. & Shen, J. R. 2003 Crystal structure of oxygen-evolving photosystem ii from thermosynechococcus vulcanus at 3.7-angstrom resolution. *Proc. Natl. Acad. Sci. USA.* **100**, 98-103.

Kok, B., Forbush, B. & McGloin, M. 1970 Cooperation of charges in photosynthetic o_2 evolution. *Photochem. Photobiol.* **11**, 457-476.

Latimer, M. J., DeRose, V. J., Mukerji, I., Yachandra, V. K., Sauer, K. & Klein, M. P. 1995 Evidence for the proximity of calcium to the manganese cluster of photosystem ii: Determination by x-ray absorption spectroscopy. *Biochemistry* **34**, 10898-10909.

Latimer, M. J., DeRose, V. J., Yachandra, V. K., Sauer, K. & Klein, M. P. 1998 Structural effects of calcium depletion on the manganese cluster of photosystem ii: Determination by x-ray absorption spectroscopy. *J. Phys. Chem. B* **102**, 8257-8265.

Loll, B., Kern, J., Saenger, W., Zouni, A. & Biesiadka, J. 2005 Towards complete cofactor arrangement in the 3.0 å resolution structure of photosystem ii. *Nature* **438**, 1040-1044.

Messinger, J., Robblee, J. H., Bergmann, U., Fernandez, C., Glatzel, P., Visser, H., Cinco, R. M., McFarlane, K. L., Bellacchio, E., Pizarro, S. A., Cramer, S. P., Sauer, K., Klein, M. P. & Yachandra, V. K. 2001 Absence of mn-centered oxidation in the s_2 to s_3 transition:Implications for the mechanism of photosynthetic water oxidation. *J. Am. Chem. Soc.* **123**, 7804-7820.

Mukerji, I., Andrews, J. C., Derose, V. J., Latimer, M. J., Yachandra, V. K., Sauer, K. & Klein, M. P. 1994 Orientation of the oxygen-evolving manganese complex in a photosystem-ii membrane preparation - an x-ray-absorption spectroscopy study. *Biochemistry* **33**, 9712-9721.

Penner-Hahn, J. E. 1998 Structural characterization of the mn site in the photosynthetic oxygen-evolving complex. *Struct. Bond.* **90**, 1-36.

Pushkar, Y., Yano, J., Glatzel, P., Messinger, J., Lewis, A., Sauer, K., Bergmann, U. & Yachandra, V. K. 2006 Structure and orientation of the mn_4ca cluster in plant photosystem ii membranes studied by polarized range-extended x-ray absorption spectroscopy. *J. Biol. Chem.* **282**, 7198-7208.

Pushkar, Y., Yano, J., Glatzel, P., Messinger, J., Lewis, A., Sauer, K., Bergmann, U. & Yachandra, V. K. 2007 Structure and orientation of the mn_4ca cluster in plant photosystem ii membranes studied by polarized range-extended x-ray absorption spectroscopy. *J. Biol. Chem.* **282**, 7198-7208.

Rutherford, A. W. 1985 Orientation of epr signals arising from components in photosystem ii membranes. *Biochim. Biophys. Acta* **807**, 189-201.

Sauer, K., Yano, J. & Yachandra, V. K. 2007 X-ray spectroscopy of the photosynthetic oxygen-evolving complex. *Coord. Chem. Rev.*, In Press.

Scott, R. A. 1984 X-ray absorption spectroscopy. In *Structural and resonance techniques in biological research* (ed. D. L. Rousseau), pp. 295-362. Orlando: Academic Press.

Scott, R. A., Hahn, J. E., Doniach, S., Freeman, H. C. & Hodgson, K. O. 1982 Polarized x-ray absorption spectra of oriented plastocyanin single crystals. Investigation of methionine-copper coordination. *J. Am. Chem. Soc.* **104**, 5364-5369.

Wydrzynski, T. & Satoh, S. 2005 *Photosystem ii: The light-driven water:Plastoquinone oxidoreductase*. Advances in photosynthesis and respiration. Dordrecht: Springer.

Yachandra, V. K. 1995 X-ray absorption spectroscopy and applications in structural biology. *Methods Enzymol.* **246**, 638-675.

Yachandra, V. K. 2005 The catalytic manganese-cluster: Organization of the metal ions. In *Photosystem ii: The light-driven water:Plastoquinone oxidoreductase*, vol. 22 (ed. T. Wydrzynski & S. Satoh), pp. 235-260. Dordrecht: Springer.

Yano, J., Kern, J., Irrgang, K.-D., Latimer, M. J., Bergmann, U., Glatzel, P., Pushkar, Y., Biesiadka, J., Loll, B., Sauer, K., Messinger, J., Zouni, A. & Yachandra, V. K. 2005a X-ray damage to the mn4ca complex in photosystem ii crystals: A case study for metallo-protein x-ray crystallography. *Proc. Natl. Acad. Sci. USA* **102**, 12047-12052.

Yano, J., Kern, J., Sauer, K., Latimer, M., Pushkar, Y., Biesiadka, J., Loll, B., Saenger, W., Messinger, J., Zouni, A. & Yachandra, V. K. 2006 Where water is oxidized to dioxygen: Structure of the photosynthetic mn_4ca cluster. *Science* **314**, 821-825.

Yano, J., Pushkar, Y., Glatzel, P., Lewis, A., Sauer, K., Messinger, J., Bergmann, U. & Yachandra, V. K. 2005b High-resolution mn exafs of the oxygen-evolving complex in photosystem ii: Structural implications for the mn_4ca cluster. *J. Am. Chem. Soc.* **127**, 14974-14975.

Yano, J. & Yachandra, V. K. 2007 Oxidation state changes of the mn_4ca cluster in photosystem ii. *Photosyn. Res.*, In Press.

Zouni, A., Witt, H.-T., Kern, J., Fromme, P., Krauß, N., Saenger, W. & Orth, P. 2001 Crystal structure of photosystem ii from *synechococcus elongatus* at 3.8 å resolution. *Nature* **409**, 739-743.

Figure Captions

Figure 1

Mn XANES and EXAFS of single crystals of photosystem II from *Thermosynechococcus elongatus* as a function of X-ray dose. As the X-ray dose increases, Mn in PS II normally present as $Mn_4(III_2,IV_2)$ is reduced to Mn(II) as seen by the changes in XANES spectra (left top). The Mn XANES from Mn complexes in formal oxidation states II, III and IV are shown in left bottom. The changes in the EXAFS spectra (right) show that the three Fourier peaks characteristic of Mn-bridging-oxo, Mn-terminal, and Mn-Mn/Ca interactions (dashed vertical line) are replaced by one Fourier peak characteristic of a Mn(II) environment. The FT marked C is from a sample given approximately the average dose in the X-ray diffraction studies. The FT on top from an intact PS II is characteristic of samples used in the X-ray spectroscopy experiment.

Figure 2

A) The structural models determined from the polarized EXAFS spectra of oriented PS II single crystals from *Thermosynechococcus elongatus*. The distance between Mn_A-Mn_B, Mn_B-Mn_C is ~2.7 Å, Mn_C-Mn_D is ~2.8 Å, and Mn_B-MnD is ~3.2 Å. There are at least two Ca-Mn distances of ~3.4 Å (Yano et al. 2006).

B) The structural models II, IIa and III are placed in the ligand environment from the X-ray diffraction data of Loll et al. at a resolution of 3.0 Å. The center of mass was translated to the center of electron density attributed to the Mn_4Ca cluster in the XRD structure without any rotation (Loll et al. 2005).

Figure 3

A) A schematic representation of the detection scheme. Mn and Fe Kα1 and Kα2. The multi-crystal monochromator with ~1 eV resolution is tuned to the Kα1 peak (red). The fluorescence peaks broadened by the Ge-detector with 150-200eV resolution are shown below (blue). Right: The PS II Mn K-edge EXAFS spectrum from the S_1 state sample obtained with a traditional energy-discriminating Ge-detector (blue) compared with that collected using the high-resolution crystal monochromator (red). Fe present in PS II does not pose a problem with the high resolution detector (the Fe edge is marked by a green line).

B) Fourier Transform (FT) of Mn K-edge EXAFS spectra from isotropic solution and oriented PS II membrane samples in the S_1, S_2 and oriented S_1 state obtained with a high-resolution spectrometer (range-extended EXAFS). Angles indicate orientation of the membrane normal with respect to the X-ray **e**-field vector. The *k* range was 3.5-15.2 $Å^{-1}$.

C) Polar plot of the X-ray absorption linear dichroism of PS II samples in the S_1 state. The N_{app} values (solid circles) for oriented membranes are plotted at their respective detection angles (θ). The best fits of N_{app} vs. θ to the equation in the text are shown for the various Mn-Mn vectors as solid lines that take into account the experimentally determined mosaic spread of Ω = 20°.

Figure 4

A) The energy level diagram for 1s2p RIXS. Excitation energy, ν, corresponding to a 1s to 3d transition, is scanned using a double crytsal monochromator; *f* is the 2p to 1s emission that is scanned using a high resolution crystal monochromator. The difference, ν-*f*, corresponds to an L-edge-like (2p to 3d) transition.

B) Contour plots of the $1s2p_{3/2}$ RIXS planes for three molecular complexes $Mn^{II}(acac)_2(H_2O)_2$, $Mn^{III}(acac)_3$, and $Mn^{IV}(sal)_2(bipy)$ and PS II in the S_1- and S_2-state. One axis is the excitation energy and the other is the energy transfer axis. The L-edge like spectra are along the energy transfer axis and the 1s to 3d transition is along the excitation energy. The assignment of $Mn(III_2,IV_2)$ for the S_1 state is confirmed by these spectra.

C) Integrated spectra along the incident energy axis, (K-edge, 1s to 3d) (right), and energy transfer axis, (L_3 edge, 2p to 3d) (left) of the contour plot shown in Fig. 4B for $Mn^{III}(acac)_3$ and $Mn^{IV}(sal)_2(bipy)$ and S_1-state of PS II. The spectra show that the Mn oxidation state of S_1 is a combination of (III) and (IV).

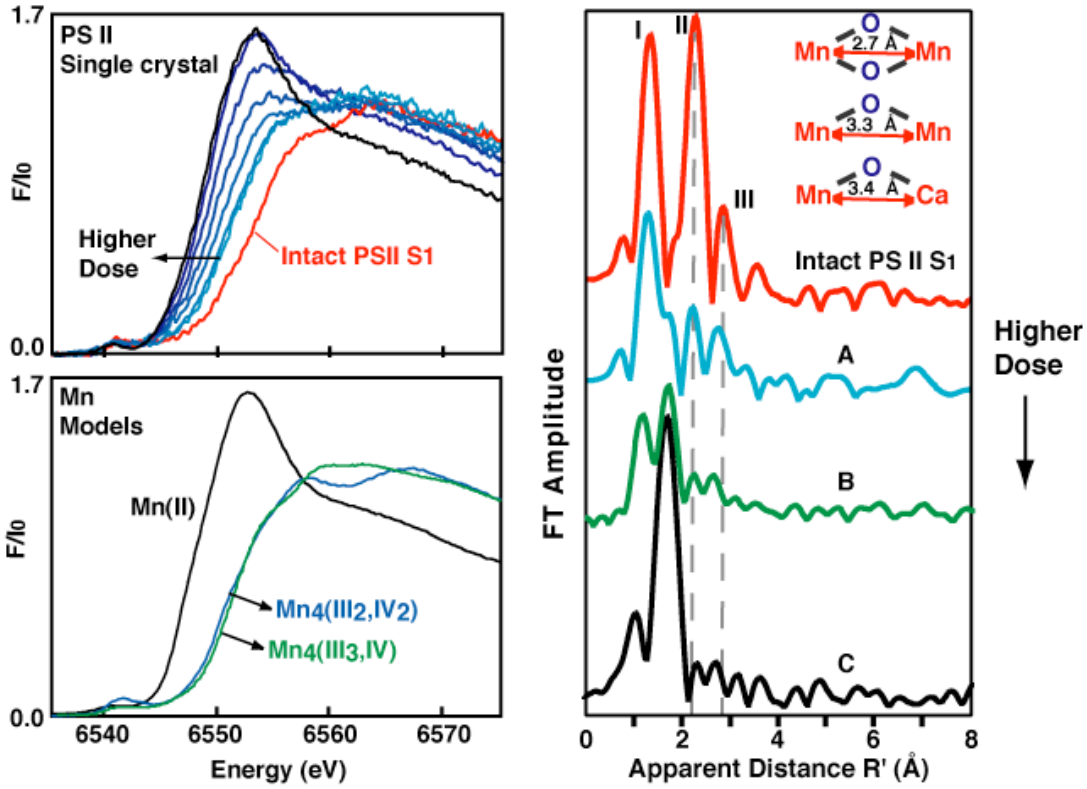
1.7
PS II
Single crystal
F/I0
Higher
Dose
Intact PSII S1
0.0
1.7
Mn
Models
Mn(II)
F/I0
Mn4(III2,IV2)
Mn4(III3,IV)
0.0
6540
6550
6560
6570
Energy (eV)
I
II
III
Mn
O
2.7 Å
Mn
Mn
O
3.3 Å
Mn
Mn
O
3.4 Å
Ca
Intact PS II S1
A
B
C
FT Amplitude
Higher
Dose
0
2
4
6
8
Apparent Distance R' (Å)

Fig. 1

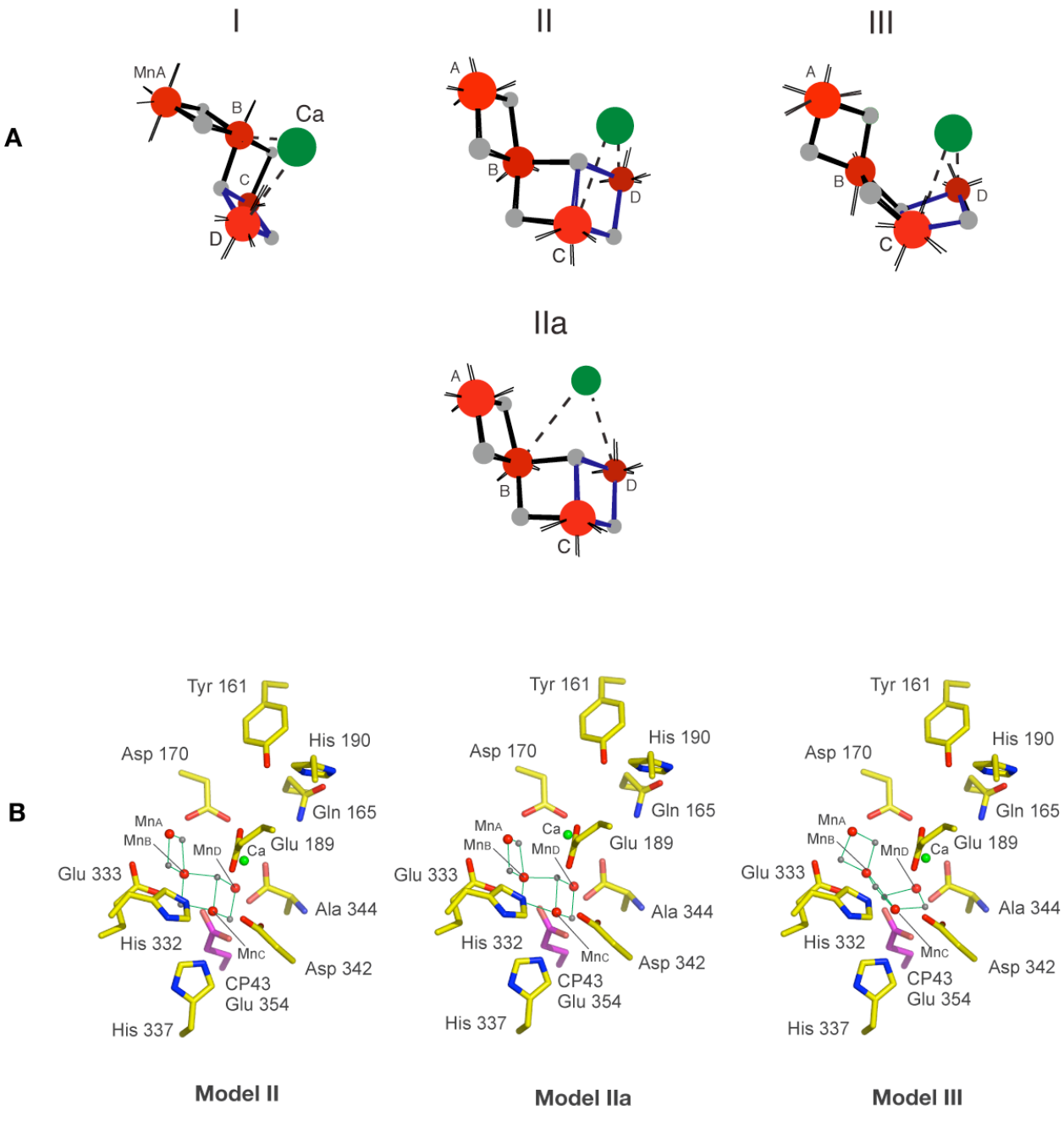
A
I
II
III
IIa
MnA
B
Ca
C
D
A
B
C
D
A
B
D
C
A
B
D
C
B
Tyr 161
His 190
Asp 170
Gln 165
MnA
MnB
MnD
Ca
Glu 189
Glu 333
Ala 344
His 332
MnC
Asp 342
CP43
Glu 354
His 337
Model II
Model IIa
Model III

Fig. 2

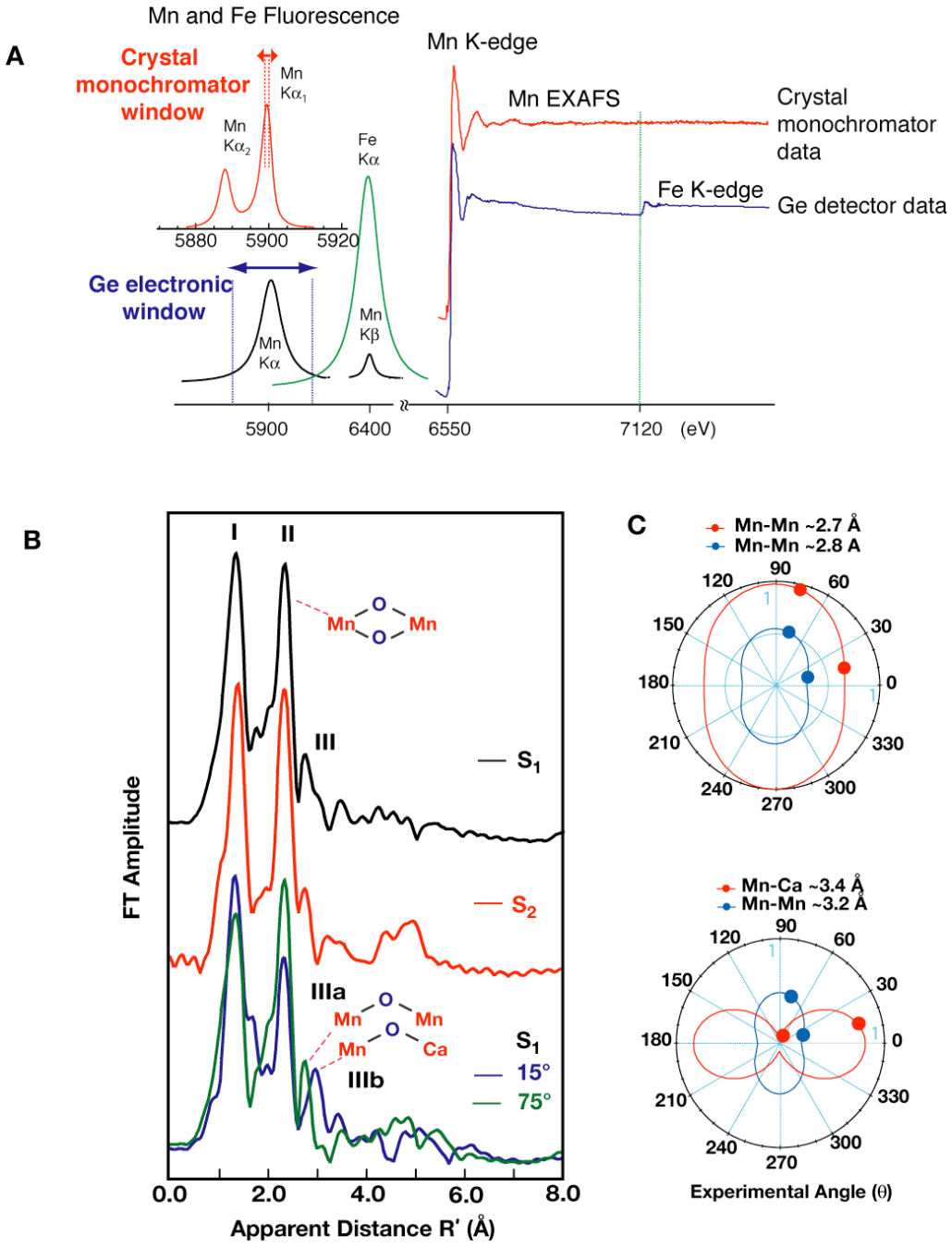
A
Mn and Fe Fluorescence
Crystal monochromator window
Mn Kα1
Mn Kα2
Fe Kα
5880
5900
5920
Ge electronic window
Mn Kα
Mn Kβ
Mn K-edge
Mn EXAFS
Fe K-edge
Crystal monochromator data
Ge detector data
5900
6400
6550
7120 (eV)
B
I
II
III
Mn
O
Mn
S1
S2
IIIa
Mn
O
Mn
Mn
O
Ca
IIIb
S1
15°
75°
FT Amplitude
0.0
2.0
4.0
6.0
8.0
Apparent Distance R' (Å)
C
Mn-Mn ~2.7 Å
Mn-Mn ~2.8 A
90
120
60
150
30
180
0
210
330
240
300
270
Mn-Ca ~3.4 Å
Mn-Mn ~3.2 Å
Experimental Angle (θ)

Fig. 3

A

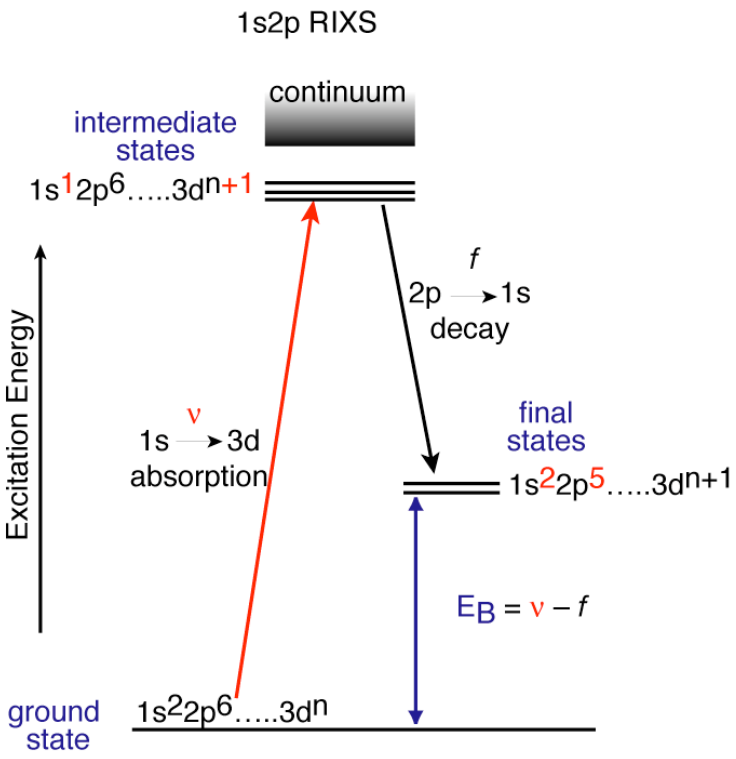
1s2p RIXS
continuum
intermediate states
1s12p6.....3dn+1
f
2p → 1s
decay
Excitation Energy
ν
1s → 3d
absorption
final states
1s22p5.....3dn+1
EB = ν – f
ground state
1s22p6.....3dn

Fig. 4

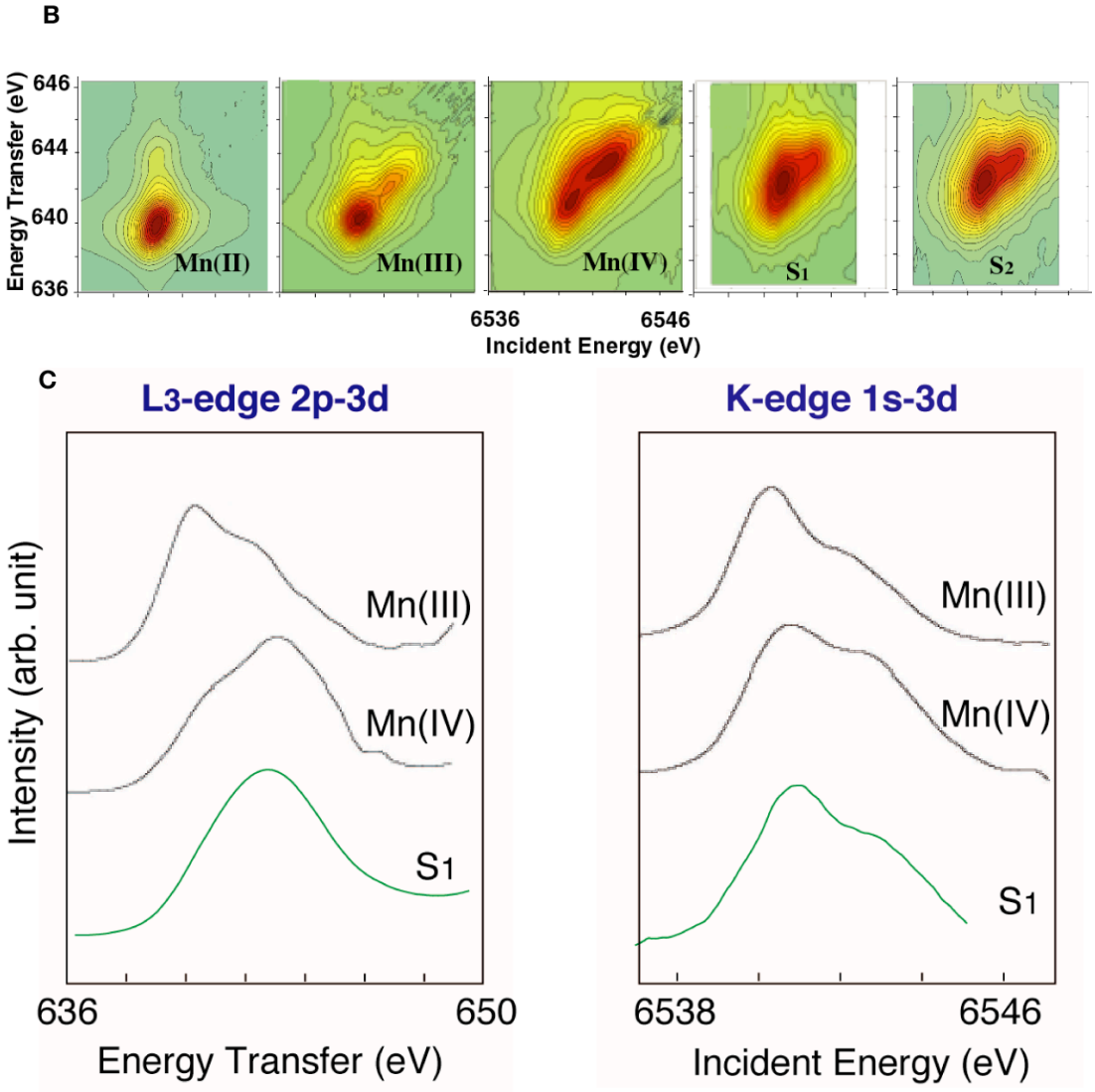
B
Energy Transfer (eV)
646
644
640
636
Mn(II)
Mn(III)
Mn(IV)
S1
S2
6536
6546
Incident Energy (eV)
C
L3-edge 2p-3d
K-edge 1s-3d
Intensity (arb. unit)
Mn(III)
Mn(IV)
S1
636
650
Energy Transfer (eV)
6538
6546
Incident Energy (eV)

Fig. 4

Answers to questions

Question by Prof. Charles Dismukes:

Do your RIXS data provide more proof for the oxidation state assignments for the Mn ions in PS II vs the earlier XANES data which rely entirely on comparison to reference model compounds.

Answer:

RIXS spectra provide a way for obtaining the effective number of electrons on Mn and also the degree of covalency. Therefore one can reliably determine the charge on the metal, which is $Mn_4(III_2,IV_2)$ in the S_1 state, and the changes between the S-states can tell us about the difference in the charge and in the degree of covalency. We find that the electron that is extracted from the OEC between S_1 and S_2 is strongly delocalized, consistent with strong covalency for the electronic configuration in the OEC. The orbital population change per change in oxidation state between the S_2 and S_3 states is half as much as that between that between S_0 and S_1, or S_1 and S_2 transitions, indicating that the electron is removed from a more covalent form or even more delocalized orbital during this transition.

Question by Prof. Ron Pace:

Is the overall dichroism seen in the EXAFS pattern greater in the oriented PS II membranes than in the rotation patterns from single crystal.

Answer:

The observed dichroism is different for the oriented PS II membranes and crystals, as expected. PS II membranes are oriented in the xy plane, and hence there is no discrimination between x and y, or +z and –z (top and bottom of the PS II membrane). On the other hand, PS II crystals are organized in three dimensions containing four molecules (PS II membranes)/unit cell, that contribute to the differences compared to oriented PSII membrabes, and also generate the complicated dichroism pattern. The other parameter that influences the dichroism is the mosaic spread, which is very small (~0.1) for crystals, but can be large (~20) for oriented PS II membranes.

Question by Prof. Jim Barber:

Although EXAFS can give high resolution spatial information for the Mn cluster, but is it correct to call your overall model of the OEC including Ca^{2+} and the amino acid residues “high resolution”? Surely the quality of model is dependent on the accuracy of the positioning of the Ca^{2+} and the amino acid side chains which at present are at intermediate resolution and perhaps modified by radiation damage.

Answer:

The structure of the Mn cluster determined from single-crystal EXAFS is at an accuracy of ~0.02 Å in distances and ~0.15 Å in resolution. Moreover, the structure of the Mn cluster is independent of the details of the PS II structure determined from the X-ray structure, or the positioning of the amino acid side chains. Therefore, we think it is justified to refer to the EXAFS-derived Mn cluster as a high resolution structure, as we are referring only to the Mn cluster, and it does not have anything to do with the overall PS II structure or the vicinity of the Mn cluster in the OEC.